

# Probing anomalous couplings using di-Higgs production in electron-proton collisions

Mukesh Kumar,<sup>1,\*</sup> Xifeng Ruan,<sup>2,†</sup> Rashidul Islam,<sup>3,‡</sup> Alan S. Cornell,<sup>1,§</sup> Max Klein,<sup>4,¶</sup> Uta Klein,<sup>4,\*\*</sup> and Bruce Mellado<sup>2,††</sup>

<sup>1</sup>*National Institute for Theoretical Physics, School of Physics,  
School of Physics and Mandelstam Institute for Theoretical Physics,  
University of the Witwatersrand, Johannesburg, Wits 2050, South Africa.*

<sup>2</sup>*University of the Witwatersrand, School of Physics, Private Bag 3, Wits 2050, South Africa.*

<sup>3</sup>*Department of Physics, University of Calcutta,  
92, Acharya Prafulla Chandra Road, Kolkata 700009, India.*

<sup>4</sup>*Oliver Lodge Laboratory, University of Liverpool, Liverpool, United Kingdom.*

A proposed high energy Future Circular Hadron-Electron Collider would provide sufficient energy in a clean environment to probe di-Higgs production. Using this channel we show that the azimuthal angle correlation between the missing transverse energy and the forward jet is a very good probe for the non-standard  $hhh$  and  $hWW$  couplings. We give the exclusion limits on these couplings as a function of integrated luminosity at 95% C.L. using the fiducial cross sections. The Higgs self-coupling could be measured to be within factors of  $0.84 (0.89) < g_{hhh}^{(1)} < 1.19 (1.12)$  of its expected Standard Model value at  $\sqrt{s} = 3.5 (5.0)$  TeV for an ultimate  $10 \text{ ab}^{-1}$  of integrated luminosity.

PACS numbers: 14.80.Ec, 11.30.Er, 13.60.-r

The new 125 GeV particle discovered by the ATLAS and CMS experiments [1–5] has been established as a spin-0 Higgs boson rather than a spin-2 particle [6, 7]. The measurements of its couplings to fermions and gauge bosons are being updated constantly and the results confirm consistency with the expected Standard Model (SM) values so far [4, 8–10]. However, to establish that a scalar doublet  $\Phi$  does indeed break the electroweak symmetry spontaneously when it acquires a nonzero vacuum expectation value,  $v$ , requires to measure directly the Higgs boson self coupling,  $\lambda$ . The minimal SM, merely on the basis of the economy of fields and interactions, assumes the existence of only one physical scalar,  $h$ , with  $J^{PC} = 0^{++}$ . Although Ref. [8] has ruled out a pure pseudoscalar hypothesis at a 99.98 % confidence limit (C.L.), the new particle can still have small CP-odd admixture to its couplings.

Theoretically, the Higgs boson self coupling appears when, as a result of electroweak symmetry breaking in the SM, the scalar potential  $V(\Phi)$  gives rise to the Higgs boson self interactions as follows:

$$V(\Phi) = \mu^2 \Phi^\dagger \Phi + \lambda (\Phi^\dagger \Phi)^2 \rightarrow \frac{1}{2} m_h^2 h^2 + \lambda v h^3 + \frac{\lambda}{4} h^4, \quad (1)$$

where  $\lambda = \lambda_{\text{SM}} = m_h^2/(2v^2) \approx 0.13$  and  $\Phi$  is an  $SU(2)_L$  scalar doublet. For a direct and independent measurement of  $\lambda$ , we need to access double Higgs boson production experimentally. However, this path is extremely challenging and requires a very high integrated luminosity to collect a substantial di-Higgs event rate and an excellent detector with powerful background rejection capabilities. On the theoretical side, we need to take into account also all vertices involved in the process that are sensitive to the presence of new physics beyond the SM

(BSM).

There are various proposals to build new, powerful high energy  $e^+e^-$ ,  $e^-p$  and  $pp$  colliders in the future. We have based our study on a *Future Circular Hadron-Electron Collider* (FCC-he) which employs the 50 TeV proton beam of a proposed 100 km circular  $pp$  collider (FCC-pp) and electrons from an Energy Recovery Linac (ERL) being developed for the *Large Hadron Electron Collider* (LHeC) [11, 12]. The design of the ERL is such that the  $e^-p$  and  $pp$  colliders operate simultaneously thus optimising the cost and the physics synergies between  $e^-p$  and  $pp$  processes. Such facilities would be potent Higgs research centres, see e.g. Ref. [13].

The choice of an ERL energy of  $E_e = 60$  to 120 GeV with an available proton energy  $E_p = 50 (7)$  TeV would provide a center of mass (c.m.s.) energy of  $\sqrt{s} \approx 3.5 (1.3)$  to 5.0 (1.8) TeV at the FCC-he (LHeC) using the FCC-pp (LHC) protons. The FCC-he would have sufficient c.m.s. energy to probe the Higgs boson self coupling via double Higgs boson production. The inclusive Higgs production cross section at the FCC-he is expected to be about five times larger than at the FCC-ee.

Fig. 1 shows Higgs boson pair production, at leading order, due to the resonant and non-resonant contributions in charged current deep inelastic scattering (CC DIS) at an  $e^-p$  collider. As seen in Fig. 1, the di-Higgs production involves  $hhh$ ,  $hWW$  and  $hhWW$  couplings. The  $hWW$  coupling will be extensively probed at the LHC. Presently, its value conforms to the value predicted by the SM [4, 8, 10]. The authors of Ref. [14] have shown the sensitivity of new physics contributions in  $hWW$  couplings at  $e^-p$  colliders through a study of the azimuthal angle correlation for single Higgs boson production in  $pe^- \rightarrow h j \nu_e$  with an excellent signal-to-background ratio based on the  $h \rightarrow b\bar{b}$  decay channel. Since we do not have

any direct measurement of the Higgs boson self coupling ( $hhh$ ) and quartic ( $hhWW$ ) coupling, there can be several possible sources of new physics in the scalar sector.

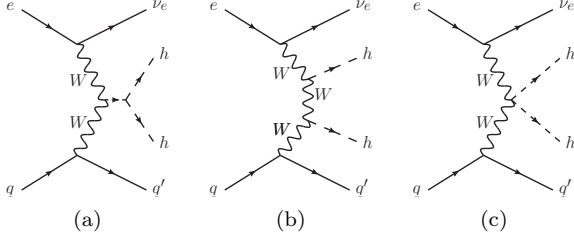


FIG. 1: Leading order diagrams contributing to the process  $p e^- \rightarrow hh j \nu_e$  with  $q \equiv u, c, \bar{d}, \bar{s}$  and  $q' \equiv d, s, \bar{u}, \bar{c}$  respectively.

This letter studies for the proposed FCC-he the sensitivity of the Higgs boson self coupling around its SM value including BSM contributions by considering all possible Lorentz structures. In order to make it a complete study we also keep the possibilities for  $hWW$  couplings that appear in the di-Higgs production modes.

Following Refs. [14, 15], the most general Lagrangian which can account for all bosonic couplings relevant for the phenomenology of the Higgs boson sector at the FCC-he are the three-point and four-point interactions involving at least one Higgs boson field. It can be written as:

$$\mathcal{L}_{hhh}^{(3)} = \frac{m_h^2}{2v} (1 - g_{hhh}^{(1)}) h^3 + \frac{1}{2} g_{hhh}^{(2)} h \partial_\mu h \partial^\mu h, \quad (2)$$

$$\begin{aligned} \mathcal{L}_{hWW}^{(3)} = & -\frac{g}{2m_W} g_{hWW}^{(1)} W^{\mu\nu} W_{\mu\nu}^\dagger h \\ & -\frac{g}{m_W} \left[ g_{hWW}^{(2)} W^\nu \partial^\mu W_{\mu\nu}^\dagger h + \text{h.c.} \right] \\ & -\frac{g}{2m_W} \tilde{g}_{hWW} W^{\mu\nu} \tilde{W}_{\mu\nu}^\dagger h, \end{aligned} \quad (3)$$

$$\begin{aligned} \mathcal{L}_{hhWW}^{(4)} = & -\frac{g^2}{4m_W^2} g_{hhWW}^{(1)} W^{\mu\nu} W_{\mu\nu}^\dagger h^2 \\ & -\frac{g^2}{2m_W^2} \left[ g_{hhWW}^{(2)} W^\nu \partial^\mu W_{\mu\nu}^\dagger h^2 + \text{h.c.} \right] \\ & -\frac{g^2}{4m_W^2} \tilde{g}_{hhWW} W^{\mu\nu} \tilde{W}_{\mu\nu}^\dagger h^2. \end{aligned} \quad (4)$$

Here  $g_{\dots}^{(i)}$ ,  $i = 1, 2$ , and  $\tilde{g}_{\dots}$  are real coefficients corresponding to the CP-even and CP-odd couplings respectively, of the  $hhh$ ,  $hWW$  and  $hhWW$  anomalous vertices. In Eq. (2)  $g_{hhh}^{(1)}$  is parametrised with a multiplicative constant w.r.t.  $\lambda_{\text{SM}}$  as in Eq. (1). Thus the Higgs self coupling  $\lambda$  appears as  $g_{hhh}^{(1)} \lambda_{\text{SM}}$  in the expression for  $V(\Phi)$ . Clearly, in the SM  $g_{hhh}^{(1)} = 1$  and all other anomalous couplings vanish in Eqs. (2)-(4). The Lorentz structures of Eqs. (2)-(4) can be derived from the  $SU(2)_L \otimes U(1)_Y$  gauge invariant dimension-6 operators given in Ref. [15].

The complete Lagrangian we work with is as follows:

$$\mathcal{L} = \mathcal{L}_{\text{SM}} + \mathcal{L}_{hhh}^{(3)} + \mathcal{L}_{hWW}^{(3)} + \mathcal{L}_{hhWW}^{(4)}. \quad (5)$$

The most general effective vertices take the form:

$$\begin{aligned} i\Gamma_{hhh} = & -6iv\lambda g_{hhh}^{(1)} \\ & -ig_{hhh}^{(2)} (p_1 \cdot p_2 + p_2 \cdot p_3 + p_3 \cdot p_1), \end{aligned} \quad (6)$$

$$\begin{aligned} i\Gamma_{hW^-W^+} = & i \left[ \left\{ \frac{g^2}{2} v + \frac{g}{m_W} g_{hWW}^{(1)} p_2 \cdot p_3 \right. \right. \\ & + \frac{g}{m_W} g_{hWW}^{(2)} (p_2^2 + p_3^2) \left. \right\} \eta^{\mu_2\mu_3} \\ & - \frac{g}{m_W} g_{hWW}^{(1)} p_2^{\mu_2} p_3^{\mu_3} \\ & - \frac{g}{m_W} g_{hWW}^{(2)} (p_2^{\mu_2} p_2^{\mu_3} + p_3^{\mu_2} p_3^{\mu_3}) \\ & \left. - i \frac{g}{m_W} \tilde{g}_{hWW} \epsilon_{\mu_2\mu_3\mu\nu} p_2^\mu p_3^\nu \right], \end{aligned} \quad (7)$$

$$\begin{aligned} i\Gamma_{hhW^-W^+} = & i \left[ \left\{ \frac{g^2}{2} + \frac{g^2}{m_W^2} g_{hhWW}^{(1)} p_3 \cdot p_4 \right. \right. \\ & + \frac{g^2}{m_W^2} g_{hhWW}^{(2)} (p_3^2 + p_4^2) \left. \right\} \eta^{\mu_3\mu_4} \\ & - \frac{g^2}{m_W^2} g_{hhWW}^{(1)} p_3^{\mu_3} p_4^{\mu_4} \\ & - \frac{g^2}{m_W^2} g_{hhWW}^{(2)} (p_3^{\mu_3} p_3^{\mu_4} + p_4^{\mu_3} p_4^{\mu_4}) \\ & \left. - i \frac{g^2}{m_W^2} \tilde{g}_{hhWW} \epsilon_{\mu_3\mu_4\mu\nu} p_3^\mu p_4^\nu \right]. \end{aligned} \quad (8)$$

The momenta and indices considered above are of the same order as they appear in the index of the respective vertex  $\Gamma$ . For example, in the vertex  $\Gamma_{hW^-W^+}$  the momenta of  $h$ ,  $W^-$  and  $W^+$  are  $p_1$ ,  $p_2$  and  $p_3$  respectively. Similarly,  $\mu_2$  and  $\mu_3$  are the indices of  $W^-$  and  $W^+$ .

In order to probe the sensitivity of these couplings we simulate the charged current double Higgs boson production channel  $p e^- \rightarrow hh j \nu_e$  (shown in Fig. 1), with  $h$  further decaying into a  $b\bar{b}$  pair, in the FCC-he set up with  $\sqrt{s} \approx 3.5$  TeV. We started our analysis optimising the SM di-Higgs signal events with respect to all possible backgrounds from multi-jet events,  $ZZ$ +jets and  $t\bar{t}$ +jets in charged and neutral current DIS and in photo-production [16], taking into account appropriate  $b$ -tagged jets and a high performance multipurpose  $4\pi$  detector. For a complete analysis see Ref. [17]. We then investigate the limits on each coupling taking BSM events as the signal. For the generation of events we use the Monte Carlo event generator **MadGraph5** [18] and the **CTEQ6L1** [19] parton distribution functions. Further fragmentation and hadronization are done with a *customised Pythia-PGS* [20, 21]. The detector level simulation is performed with reasonably chosen parameters using **Delphes** [22, 23]. The factorization and renormalisation scales for the signal simulation are fixed to the Higgs boson mass,  $m_h = 125$  GeV. The background simulations are done with the default **MadGraph5** dynamic scales. The  $e^-$  polarisation is assumed to be  $-80\%$ .

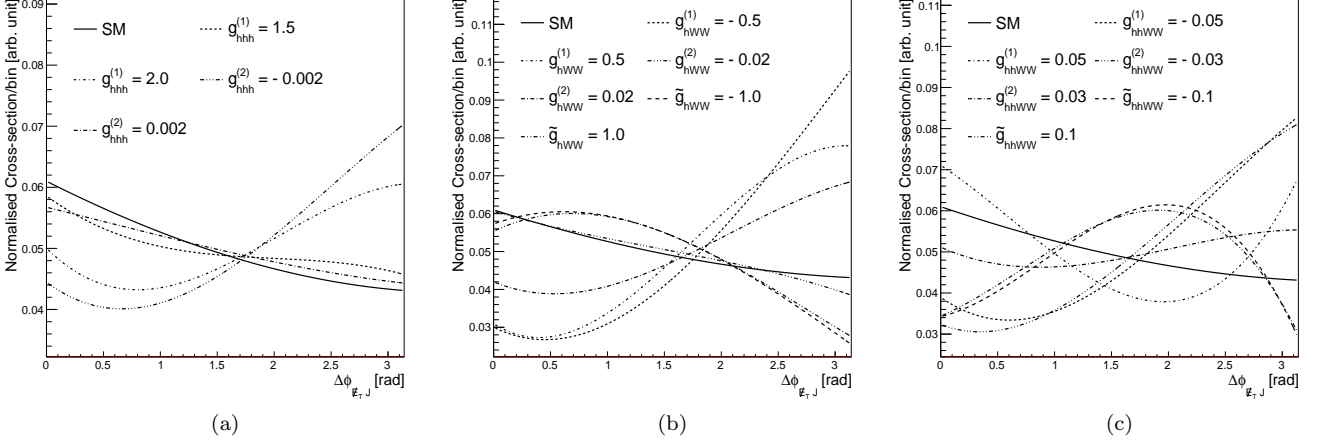


FIG. 2: Azimuthal angle distributions, at **Delphes** detector-level, between missing transverse energy,  $\cancel{E}_T$ , and the forward jet,  $J$ , in the SM and with the anomalous  $hhh$ ,  $hWW$  and  $hhWW$  couplings.

We base our simulation on the following kinematic selections in order to optimise the significance of the SM signal over all the backgrounds: (1) At least four  $b$ -tagged jets and one additional light jet are selected in an event with transverse momenta,  $p_T$ , greater than 20 GeV. (2) For *non-b*-tagged jets, the absolute value of the rapidity,  $|\eta|$ , is taken to be less than 7, whereas for  $b$ -tagged jets it is less than 5. (3) The four  $b$ -tagged jets must be well separated and the distance between any two jets, defined as  $\Delta R = \sqrt{(\Delta\phi)^2 + (\Delta\eta)^2}$ ,  $\phi$  being the azimuthal angle, is taken to be greater than 0.7. (4) Leptons with  $p_T > 10$  GeV are rejected. (5) For the largest  $p_T$  forward jet  $J$  (the *non-b*-tagged jet after selecting at least four  $b$ -jets)  $\eta_J > 4.0$  is required. (6) The missing transverse energy,  $\cancel{E}_T$ , is taken to be greater than 40 GeV. (7) The azimuthal angle between  $\cancel{E}_T$  and the jets are:  $\Delta\Phi_{\cancel{E}_T, \text{leading jet}} > 0.4$  and  $\Delta\Phi_{\cancel{E}_T, \text{subleading jet}} > 0.4$ . (8) The four  $b$ -tagged jets are grouped into two pairs w.r.t. their invariant masses. The first pair is required to be within 90-125 GeV and the second pair within 75-125 GeV. (9) The invariant mass of all four  $b$ -tagged jets has to be greater than 280 GeV. In the selections the  $b$ -tagging efficiency is assumed to be 70%, with fake rates from  $c$ -initiated jets and light jets to the  $b$ -jets of 10% and, 1% respectively.

For our analysis we take *ad hoc* values of positive and negative couplings in such a manner that the production cross section does not deviate much from the SM value, and in particular modifications in the shapes in the normalised azimuthal angle distribution between the missing transverse energy and the leading (forward) jet are studied in addition to other kinematic distributions.

Taking into account all the above criteria we study BSM modifications in various differential distributions at the **Delphes** detector-level that lead to the following ob-

servations: (1)  $p_T$  has the usual tail behavior, i.e. the number of events are more populated in the higher  $p_T$  region with respect to the SM for the chosen values of the anomalous couplings. (2) In cases of the  $\eta$  distributions: (a) For the forward jet, particularly for the couplings of  $hWW$  and  $hhWW$  vertices, the mean  $\eta$  is more central in the detector. The behavior is similar if we increase the c.m.s. energy of the collider by increasing  $E_e$  to higher ( $>60$  GeV) values. For  $hhh$  couplings the  $\eta$  distribution remains the same as for the SM. (b) In case of  $b$ -tagged jets, for all values of anomalous couplings, the distribution is populated around the value of  $\eta$  of the SM distribution. (3) For our specific observable, namely the azimuthal angle difference between missing transverse energy and the forward jet ( $\Delta\phi_{\cancel{E}_T, J}$ ) the shapes are clearly distinguishable from the SM. This behavior is shown in Fig. 2, and will be discussed in the following.

The values of the couplings taken in Fig. 2 are *ad hoc*. However, these values are taken only for the purpose of illustration, and in the limit of the couplings going to their SM values the shapes will coincide with the SM distributions. The specific characteristics of the curves also depend on the details of the selection requirements, but the qualitative differences could be seen at every selection step. Hence we conclude that  $\Delta\phi_{\cancel{E}_T, J}$  is a good observable to search for any new physics contribution to these vertices.

Furthermore, we probe the exclusion limits on these couplings as a function of the integrated luminosity, with the log-likelihood method described in Ref. [24], using directly the fiducial inclusive cross section as an observable. In Fig. 3 we present exclusion plots at 95% C.L. for anomalous  $hhh$ ,  $hWW$  and  $hhWW$  couplings, where the shaded areas are the allowed region. The exclusion limits are based on the SM ‘di-Higgs signal + backgrounds’

hypotheses considering BSM contributions as the signal at the given luminosity. Each limit is given by scanning one coupling and fixing the other couplings to their SM value, where a 5% systematic uncertainty is taken into account on the signal and background yields respectively.

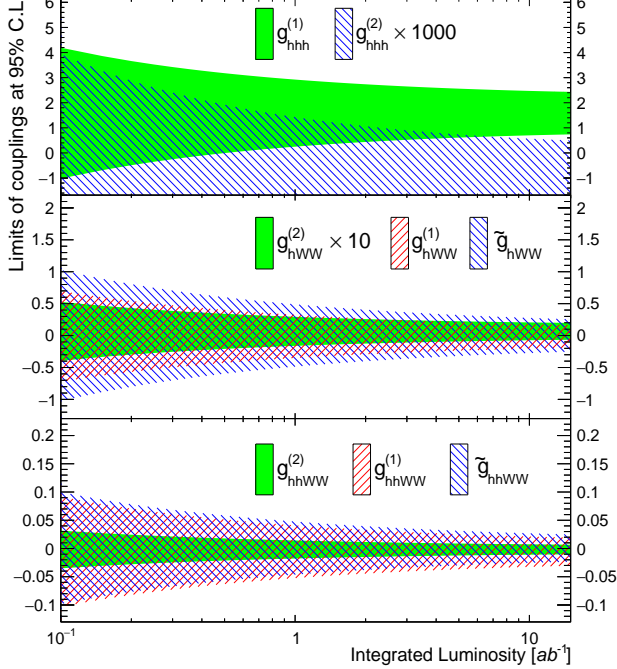


FIG. 3: The exclusion limits on the anomalous  $hhh$  (top panel),  $hWW$  (middle panel) and  $hhWW$  (lower panel) couplings at 95% C.L. as a function of integrated luminosity. The shaded areas represents values allowed still. Note that the allowed values of  $g_{hhh}^{(2)}$  ( $g_{hWW}^{(2)}$ )  $\sim 10^{-3}$  ( $10^{-1}$ ) are multiplied by  $10^3$  ( $10^1$ ).

From Fig. 3 our observations are as follows: (1) If the integrated luminosity exceeds  $0.5 \text{ ab}^{-1}$   $g_{hhh}^{(1)}$  is restricted to be positive.  $g_{hhh}^{(1)}$  is allowed to be within 0.7 to 2.4 when the integrated luminosity reaches  $15 \text{ ab}^{-1}$ . This is because for the values  $1 < g_{hhh}^{(1)} \leq 2.1$  the cross section is smaller than the SM di-Higgs production. (2) The  $g_{hhh}^{(2)}$  value is restricted to around  $10^{-3}$ , due to its significantly increasing production cross section as a function of the coupling strength. We only exclude the positive part of this coupling because its negative part has cancellations with the SM di-Higgs cross section. (3) The sensitivity for  $hWW$  couplings, namely  $g_{hWW}^{(1)}$  and  $\tilde{g}_{hWW}$  can be better probed at much lower energies and luminosity at LHeC using the single Higgs boson production as shown in Ref. [14]. However we have shown the sensitivity of  $g_{hWW}^{(2)}$ , which is not considered in Ref. [14], and it is of the order  $10^{-2}$  in the allowed region. (4) One important aspect of di-Higgs production in this type of collider is that one can measure the sensitivity of the  $hhWW$

couplings also. In our analysis, since the CP-even (odd) coupling  $g_{hhWW}^{(1)}$  ( $\tilde{g}_{hhWW}$ ) has similar Lorentz structures, the sensitivity in the exclusion plot has almost the same order of magnitude. However, the structure of  $g_{hhWW}^{(2)}$  allows a comparatively narrower region of values. The couplings belonging to both the  $hWW$  and  $hhWW$  vertices are strongly constrained because of their high production cross section at very low values of the couplings. With increasing the luminosity from  $0.1\text{--}1 \text{ ab}^{-1}$  the constraint on the couplings increases and its limits are reduced by a factor two. A further increase of the luminosity will be not change the results. All limits are derived by varying only one coupling at a time as mentioned earlier.

Finally we discuss what happens once the electron energy  $E_e$  could be increased to higher values where we focus our analysis on a determination of the SM Higgs self-coupling assuming no further BSM contributions. Without going into detail we can mention that with increasing  $E_e$  from 60 GeV to 120 GeV the SM signal and dominant background production cross sections are enhanced by factor 2.2 and 1.7 respectively. As a result, the cut efficiency for the selection of four  $b$ -tagged jets and one forward jet is improved, but for the other cuts described previously (invariant mass,  $\cancel{E}_T$ ,  $\eta_J$  and  $\Delta\phi_{\cancel{E}Tj}$ ) it remains very similar. This leads to an enhancement of the selected signal and dominant background events by a factor 2.5 and 2.7 respectively. Hence we would get the same statistical precision with only 40% of the luminosity of an  $E_e = 60 \text{ GeV}$  beam when increasing the electron energy to 120 GeV. At an ultimate integrated luminosity of  $10 \text{ ab}^{-1}$ , increasing  $E_e$  from 60 to 120 GeV would increase the significance of the observed SM di-Higgs events from 8.3 to 11.9, obtained from log-likelihood fit. This includes a 5% signal and background systematics mentioned earlier. For the SM Higgs boson self coupling where the scaling factor is expected to be  $g_{hhh}^{(1)} = 1$ , we observe that the measurement of  $g_{hhh}^{(1)}$  varies from  $0.84 < g_{hhh}^{(1)} < 1.19$  for  $E_e = 60 \text{ GeV}$  to  $0.89 < g_{hhh}^{(1)} < 1.12$  for  $E_e = 120 \text{ GeV}$ .

Overall we conclude that at the FCC-he the di-Higgs production is significant and through this channel one can probe accurately the Higgs boson self coupling along with anomalous  $hhWW$  contributions, provided that integrated luminosities of more than  $1 \text{ ab}^{-1}$  may be achieved.

We acknowledge fruitful discussions within the LHeC Higgs group, especially with Masahiro Kuze and Masahiro Tanaka. RI acknowledges the DST-SERB supported research project SRIS2/HEP-13/2012 for partial financial support.

\* Electronic address: [mukesh.kumar@cern.ch](mailto:mukesh.kumar@cern.ch)

† Electronic address: [xifeng.ruan@cern.ch](mailto:xifeng.ruan@cern.ch)

‡ Electronic address: [rashidul.islam@cern.ch](mailto:rashidul.islam@cern.ch)

- § Electronic address: [alan.cornell@wits.ac.za](mailto:alan.cornell@wits.ac.za)
- ¶ Electronic address: [Max.Klein@liverpool.ac.uk](mailto:Max.Klein@liverpool.ac.uk)
- \*\* Electronic address: [Uta.Klein@liverpool.ac.uk](mailto:Uta.Klein@liverpool.ac.uk)
- †† Electronic address: [bruce.mellado.garcia@cern.ch](mailto:bruce.mellado.garcia@cern.ch)
- [1] ATLAS Collaboration, Phys. Lett. B **716**, 1 (2012).
- [2] CMS Collaboration, Phys. Lett. B **716**, 30 (2012).
- [3] ATLAS Collaboration, Phys. Rev. D **90**, 052004 (2014).
- [4] CMS Collaboration, Eur. Phys. J. C **75**, 212 (2015).
- [5] ATLAS and CMS Collaborations, Phys. Rev. Lett. **114**, 191803 (2015).
- [6] CMS Collaboration, Phys. Rev. Lett. **110**, 081803 (2013).
- [7] ATLAS Collaboration, Phys. Lett. B **726**, 120 (2013).
- [8] CMS Collaboration, Phys. Rev. D **92**, 012004 (2015).
- [9] ATLAS Collaboration, arXiv:1506.05669 [hep-ex].
- [10] ATLAS Collaboration, arXiv:1507.04548 [hep-ex].
- [11] LHeC Study Group Collaboration, J. Phys. G **39**, 075001 (2012). <http://lhec.web.cern.ch/>
- [12] O. Bruening and M. Klein, Mod. Phys. Lett. A **28**, 1330011 (2013).
- [13] LHeC Study Group Collaboration, arXiv:1211.5102 [hep-ex].
- [14] S. S. Biswal, R. M. Godbole, B. Mellado and S. Raychaudhuri, Phys. Rev. Lett. **109**, 261801 (2012).
- [15] A. Alloul, B. Fuks and V. Sanz, JHEP **1404**, 110 (2014).
- [16] We cross checked the modelling of photo-production cross sections from **MadGraph5** by switching on the “Improved Weizsäcker-Williams approximation formula” described in Ref. [25] to give the probability of photon from the incoming electron, versus the expectation of the **Pythia** Monte Carlo generator.
- [17] M. Kumar, X. Ruan, R. Islam, A. S. Cornell, M. Klein, U. Klein and B. Mellado, In preparation.
- [18] J. Alwall, M. Herquet, F. Maltoni, O. Mattelaer and T. Stelzer, JHEP **1106**, 128 (2011).
- [19] J. Pumplin, D. R. Stump, J. Huston, H. L. Lai, P. M. Nadolsky and W. K. Tung, JHEP **0207**, 012 (2002).
- [20] T. Sjostrand, S. Mrenna and P. Z. Skands, JHEP **0605**, 026 (2006).
- [21] In **Pythia-PGS** we modified several parameters in a way to use it for  $e^-p$  collision and to get all required number of events demanded in simulation. The coordinate system is set as for the HERA experiments, i.e. the proton direction defines the forward direction. The modifications have been successfully validated using neutral current DIS events and switched off QCD ISR. For  $e^-p$  collisions multiple interactions and pile-up are expected to be very small and are switched off in our studies.
- [22] J. de Favereau *et al.* [DELPHES 3 Collaboration], JHEP **1402**, 057 (2014).
- [23] For **Delphes**, we used the ATLAS set-up with the modifications in the  $|\eta|$  ranges for forward and  $b$ -tagged jets up to 7 and 5 respectively with 70% tagging efficiency of  $b$ -jets as mentioned in the text. The resolution parameters for energy deposits in the calorimeters are based on the ATLAS Run-1 performance.
- [24] G. Cowan, K. Cranmer, E. Gross and O. Vitells, Eur. Phys. J. C **71**, 1554 (2011) [Eur. Phys. J. C **73**, 2501 (2013)].
- [25] V. M. Budnev, I. F. Ginzburg, G. V. Meledin and V. G. Serbo, Phys. Rept. **15** (1975) 181.